Supplementary Figures

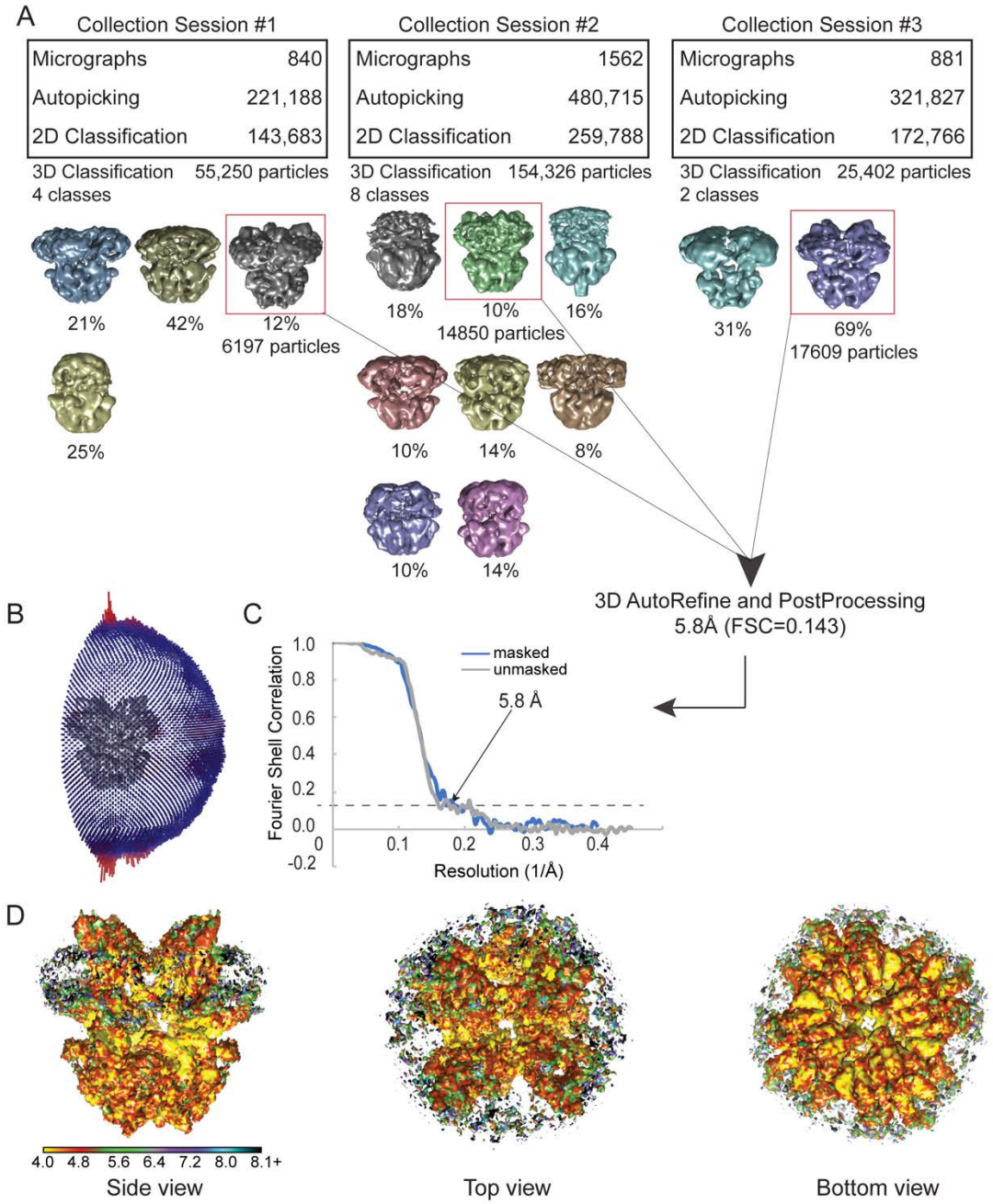

Supplementary figure 1. Flowchart for $TRPC3_{GDN}$ image processing pipeline.
A. Flowchart showing the number of micrographs, autopicked particles, and particles that went into 2D and 3D classification steps. All 3D class averages are shown with percentage of particles they contain underneath. Averages whose particles were used in 3D autorefine and post-processing are boxed in red. **B.** Angular distribution of views that went into the final reconstruction of $TRPC3_{GDN}$. **C.** Fourier shell correlation (FSC) curve for $TRPC3_{GDN}$ data taken on the Polara microscope showing a 5.8 Å resolution cut-off at the gold standard value of 0.143. **D.** Side, top, and bottom views of TRPC3 with local resolution indicated in the heat map scale bar under the side view. High to low resolution runs yellow to black, with a scale from 4.0-8.0 Å.

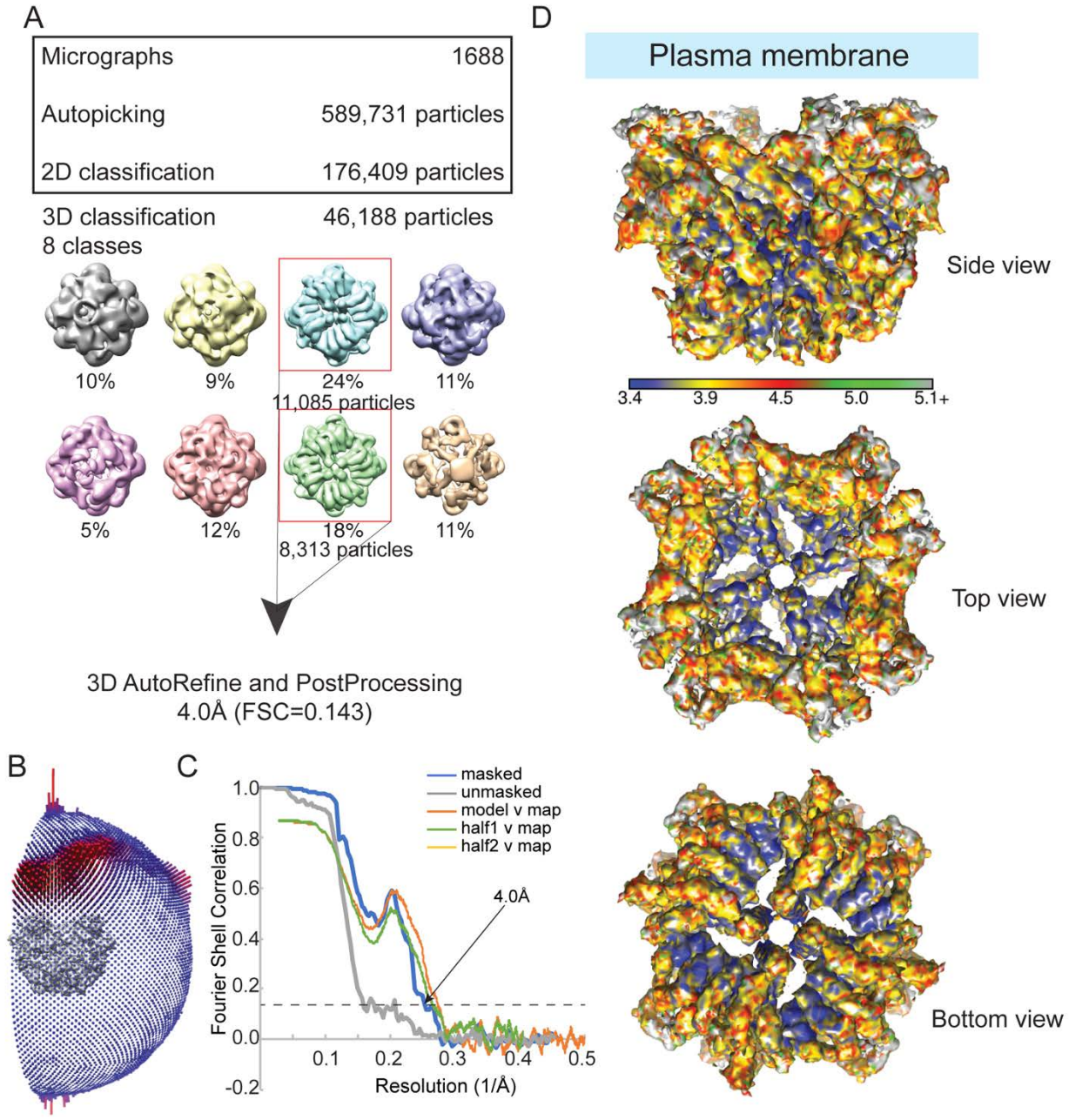

Supplementary figure 2. Flowchart for TRPC3$_{PMAL}$ image processing pipeline.
A. Flowchart showing the number of micrographs, autopicked particles, and particles that went into 2D and 3D classification steps. All 3D class averages are shown with percentage of particles they contain underneath. Averages whose particles were used in 3D autorefine and post-processing are boxed in red. **B.** Angular distribution of views that went into the final reconstruction of TRPC3$_{PMAL}$. **C.** Fourier shell correlation (FSC) curve for TRPC3$_{PMAL}$ data (blue) and TRPC3 model (orange) taken showing a 4.0Å resolution cut-off at the gold standard value of 0.143. **D.** Side, top, and bottom views of TRPC3$_{PMAL}$ with local resolution indicated in the heat map scale bar under the side view. High to low resolution runs blue to green, with a scale from 3.4-5.1 Å.

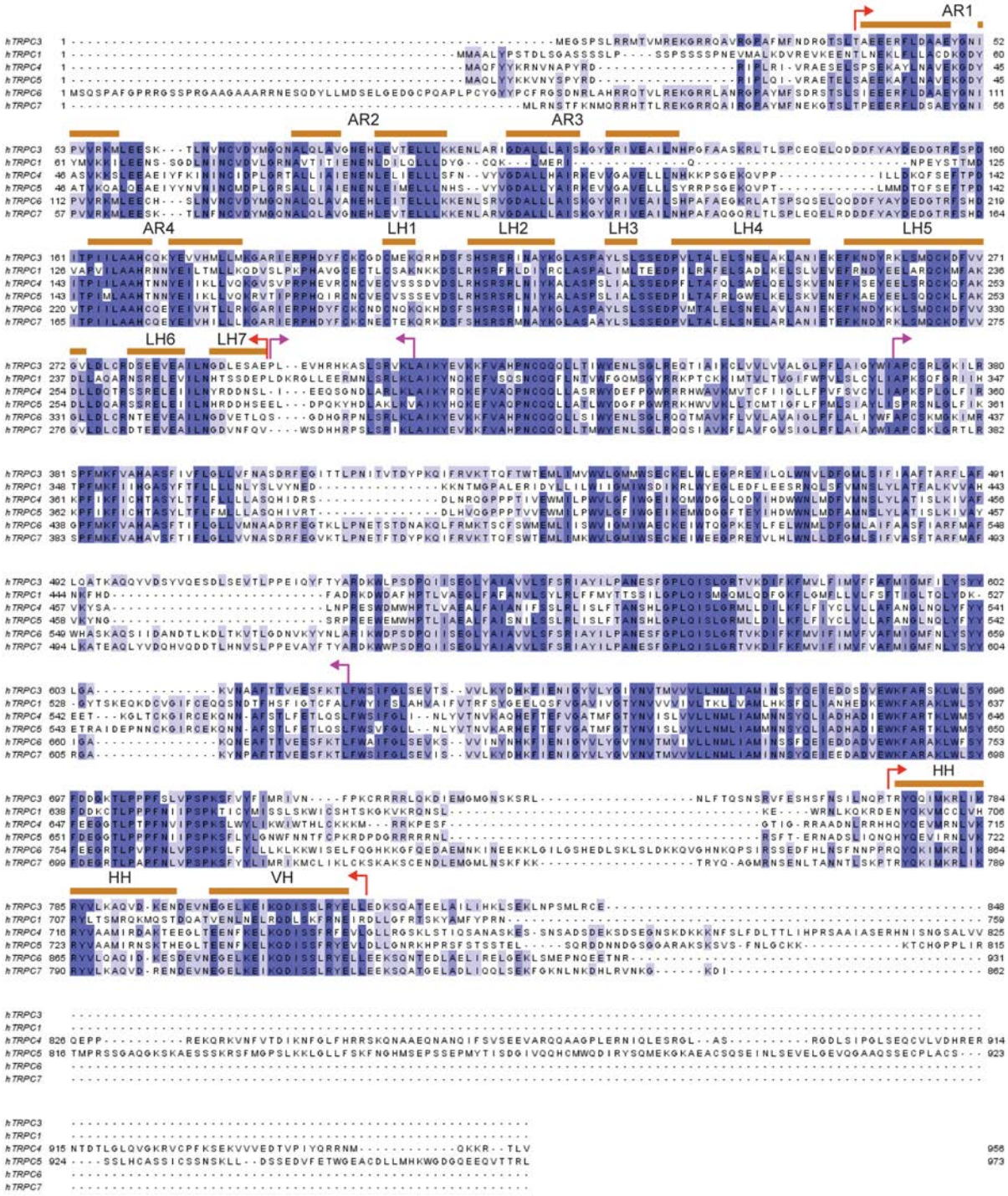

Supplementary figure 3. Sequence alignment of human TRPC channels.
The sequences for hTRPC1/3/4/5/6/7 were aligned using the Clustal Omega program and colored using percentage of identity score in Jalview v2 (Waterhouse et al., 2009). Secondary structure assignments are based on our human TRPC3 structure with α-helices indicated in orange. Red arrows indicate the CPD model built with side-chains, and magenta arrows indicate the polyalanine model built of the TMD.

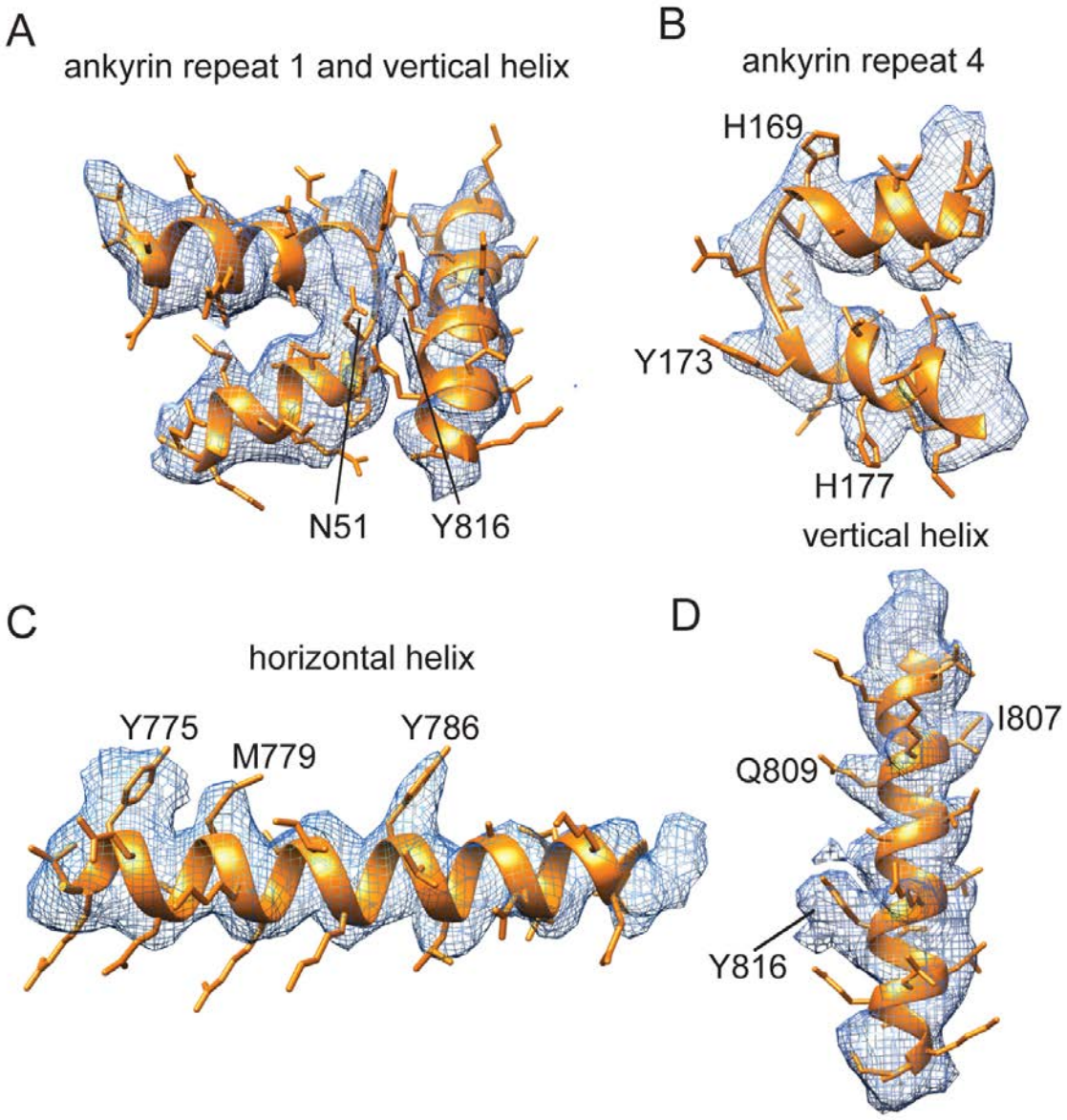

Supplementary figure 4. Representative regions for local fit of the atomic model of TRPC3$_{PMAL}$ cytoplasmic domain in the 4.0Å density map determined on the Titan Krios.
A. Ankyrin repeat 1 and part of the vertical helix, showing contact between N51 and Y816. **B.** Ankyrin repeat 4. **C.** C-terminal horizontal helix. **D.** C-terminal vertical helix.

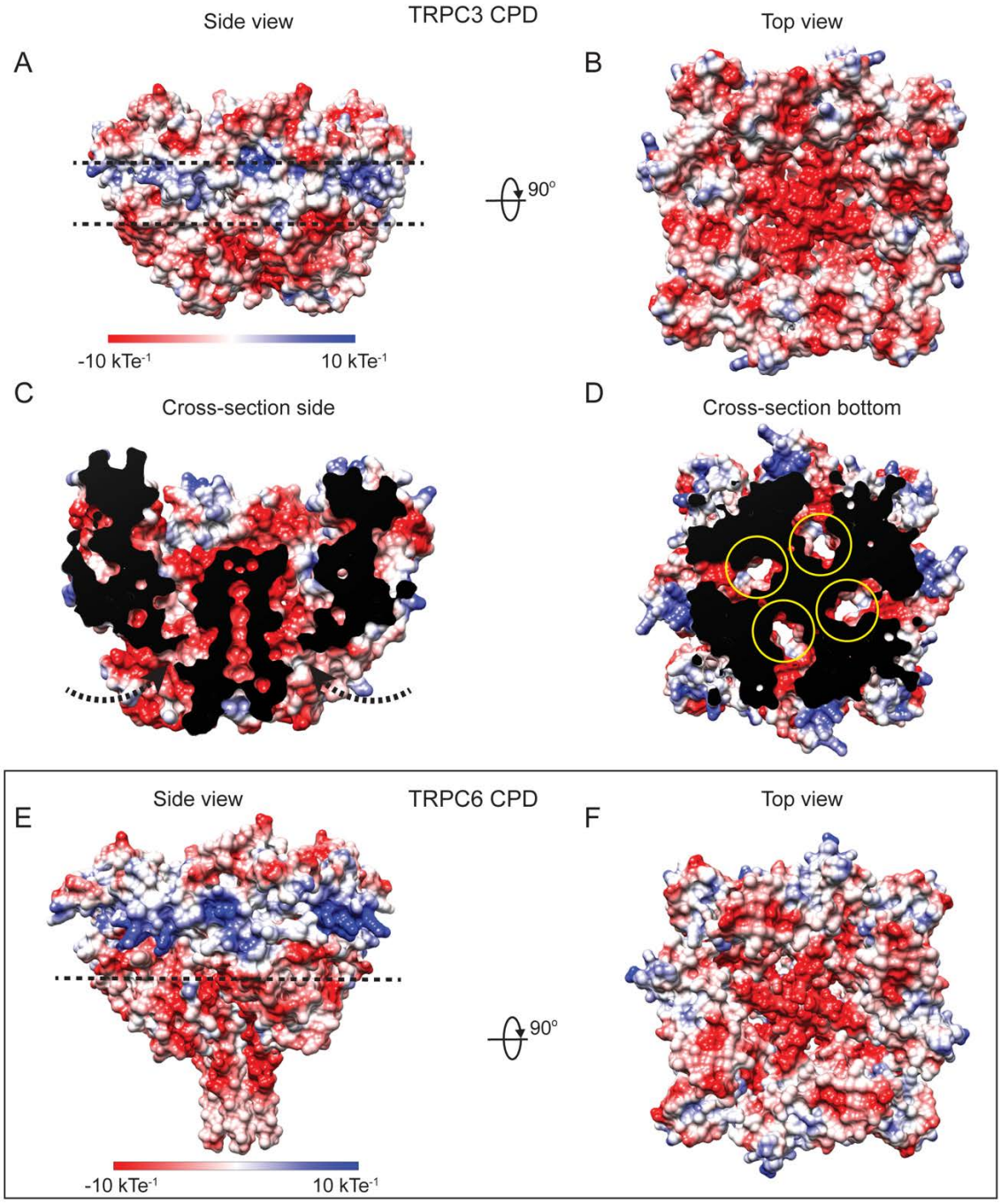

Supplementary figure 5. Electrostatic potential of TRPC3$_{PMAL}$ cytoplasmic domain.
A. Side view indicating the sandwich-like distribution of negative, neutral, and positive charges on the CPD surface. Dotted lines indicate a patch of neutral and positive charges. **B.** Top view indicating the overall negative charge of the inner chamber. **C.** Side view cross-section indicating the openings that provide access to the chamber interior (arrow). **D.** Top view cross-section showing the openings that connect the cytoplasm to the bowl interior and channel gate (yellow circles). **E.** Side view of the TRPC6 CPD indicating the dual distribution of negative and neutral, and positive charges on the CPD surface. Dotted line indicates the boundaries of the electrostatic potential. **F.** Top view indicating the overall negative charge of the TRPC6 inner chamber.

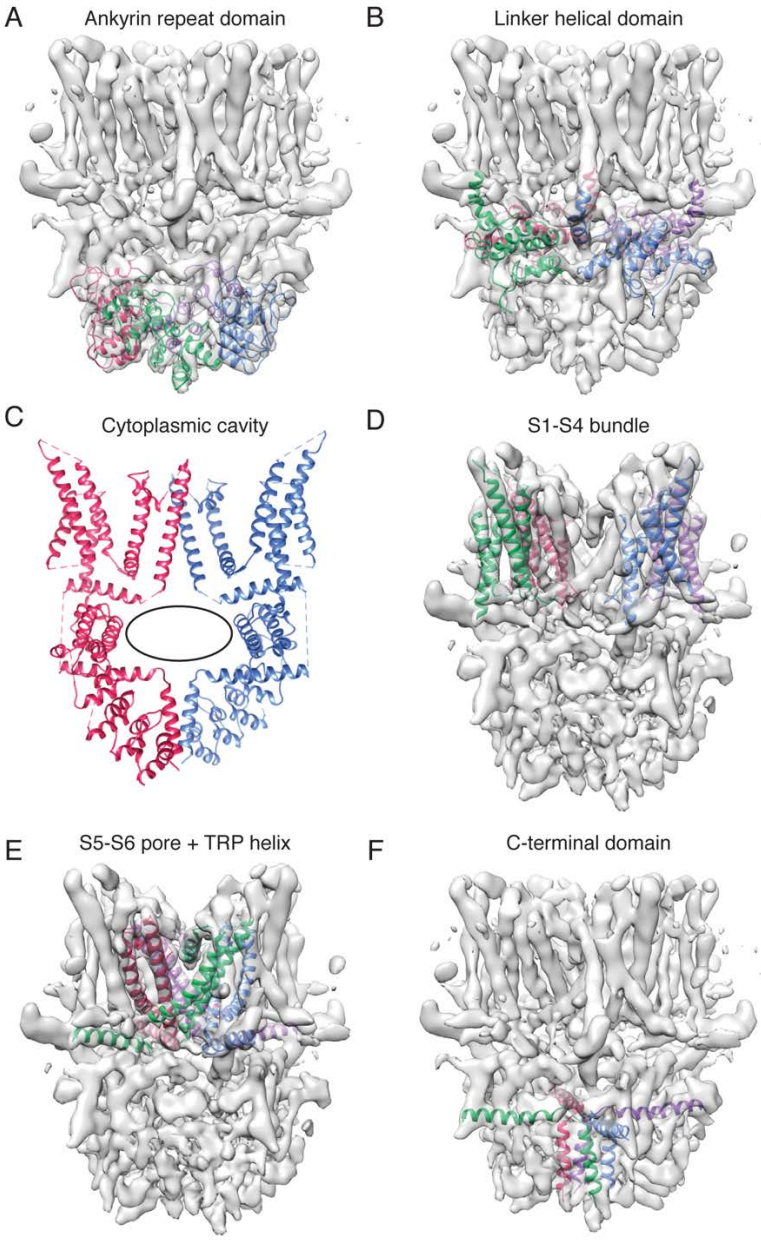

Supplementary figure 6. Layered organization of TRPC3.
A. Electron density map of $TRPC3_{GDN}$ is represented in transparent grey with only the ankyrin repeat domains of the four subunits shown and colored in blue, green, pink, and purple. These form the base of the inverted dome of the CPD. **B.** The linker helical domains of the four subunits are shown in the $TRPC3_{GDN}$ electron density map forming the top of the inverted dome of the CPD. **C.** Two, opposite subunits of TRPC3 are show in pink and blue to highlight the inner chamber (black oval) formed by the CPD that sits underneath the transmembrane helices. **D.** The S1-S4 transmembrane helix bundle of the four subunits shown and colored in blue, green, pink, and purple inside the $TRPC3_{GDN}$ electron density map. **E.** Electron density map of $TRPC3_{GDN}$ is represented in transparent grey with the S5-S6 pore helices, including the TRP helix, of the four subunits shown and colored in blue, green, pink, and purple. **F.** The C-terminal horizontal and vertical helices of the four subunits shown in the $TRPC3_{GDN}$ electron density map coming in from the sides of the dome and forming a coiled coil.

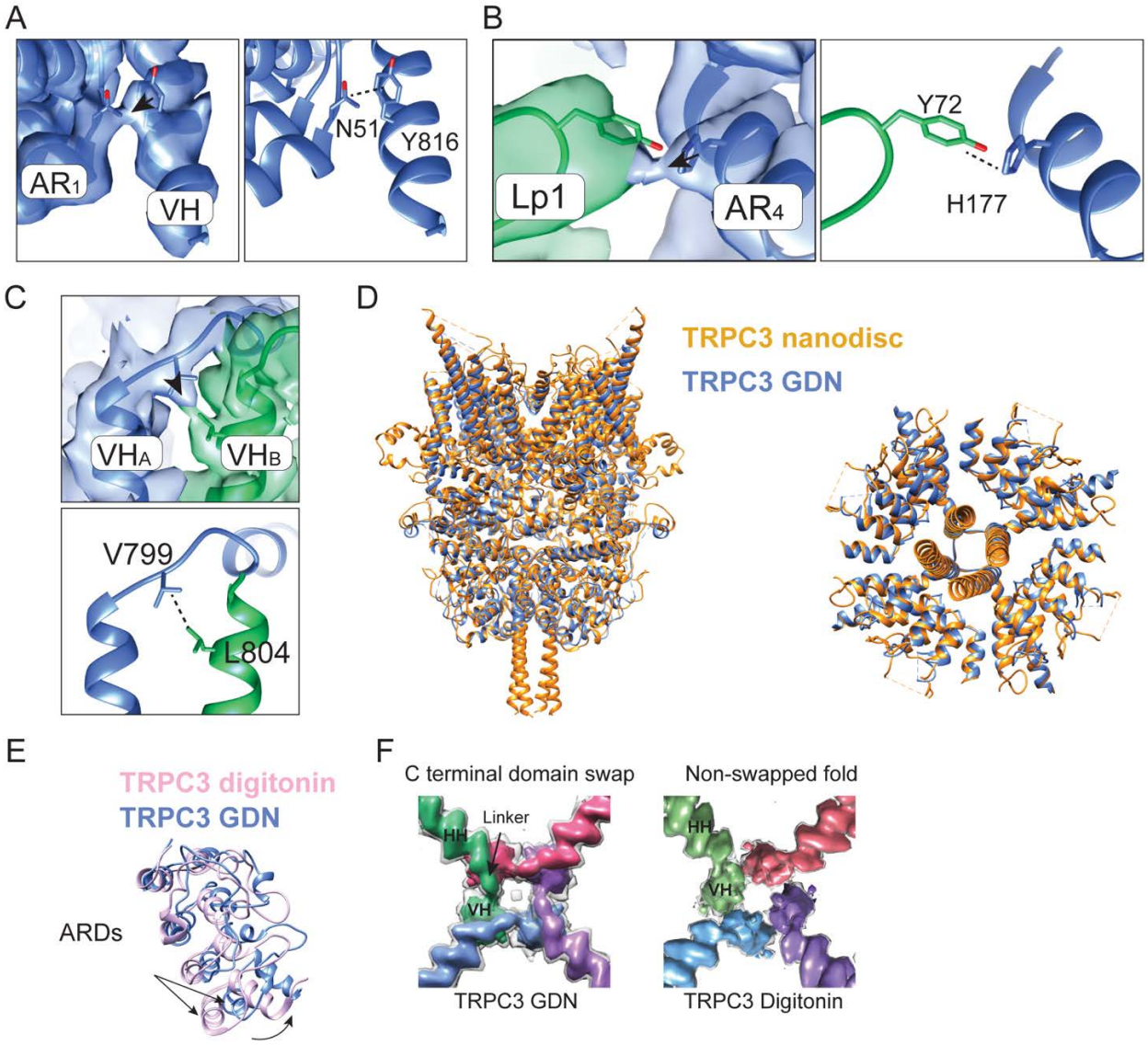

Supplementary figure 7. Cytoplasmic domain α-helix interactions.
A. Inter-subunit interactions between the VH and AR1. Map is presented at σ28 with sigma calculated as the map threshold divided by the RMS calculated in UCSF Chimera. **B.** Intra-subunit interactions between the loop between AR1 and AR2 (green) and the adjacent subunit's AR4 (blue). Maps are presented at σ19 and σ20. **C.** Intra-subunit interactions between adjacent VHs. Both maps are presented at σ17. **D.** Left: side view superposition of full length $TRPC3_{GDN}$ (blue) and $TRPC3_{nanodisc}$ (orange) and right: bottom view superposition of the CPD. **E.** Superposition of AR1-4 between the $TRPC3_{GDN}$ (blue) and $TRPC3_{digitonin}$ (pink) structures showing that AR1-3 are shifted counter-clockwise in $TRPC3_{GDN}$. Black arrows indicate the change in position between the ankyrin repeats. **F.** Electron density maps highlighting the intersection of the HHs and VHs of $TRPC3_{GDN}$ (domain swap) and $TRPC3_{digitonin}$ (no domain swap; EMD-7620). Individual subunits colored in blue, green, pink, and purple are displayed at a higher threshold than the tetramer in transparent grey.

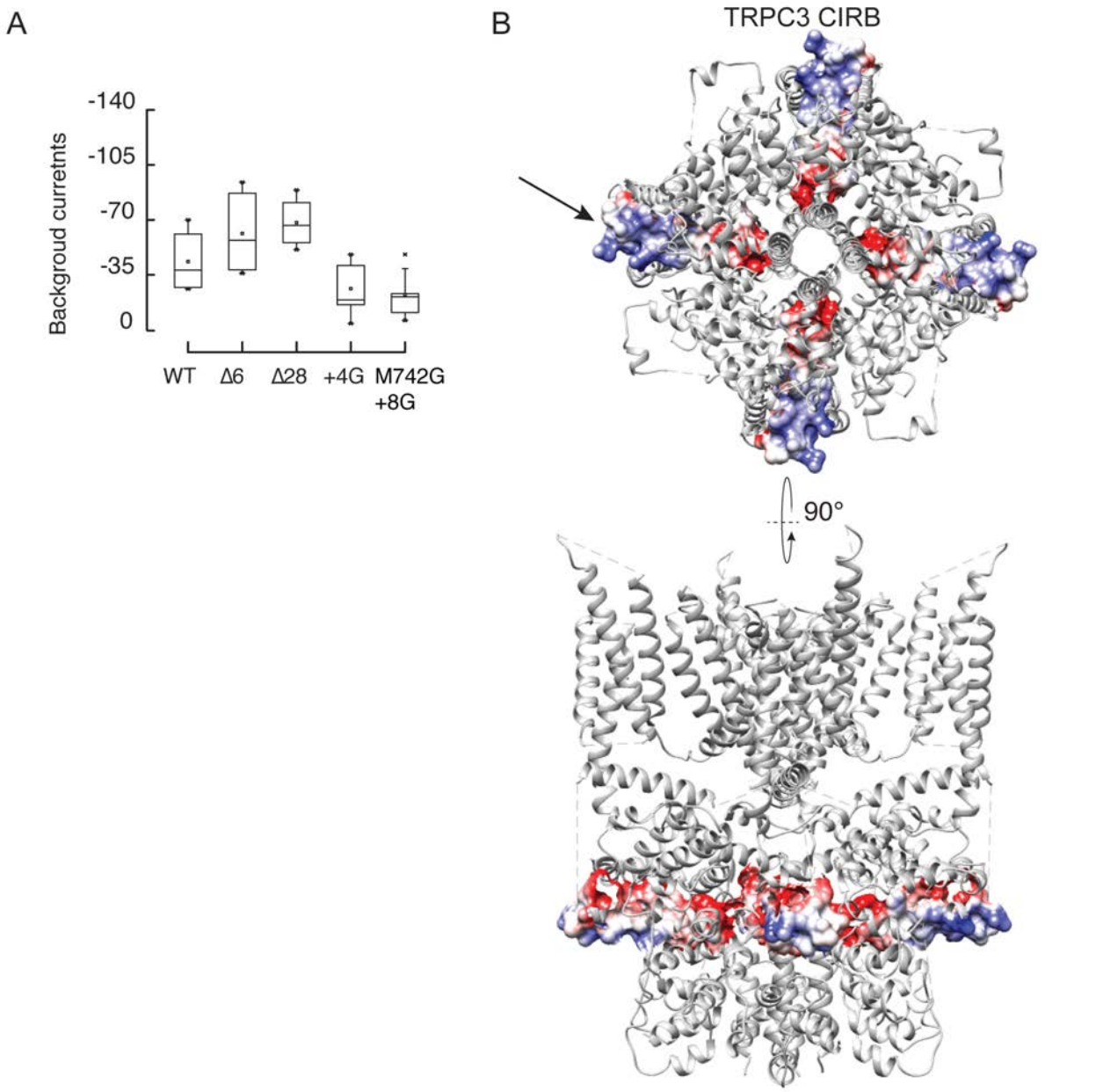

Supplementary figure 8. Effects of the C-terminal loop and CIRB domain on TRPC3 gating. **A.** Background currents for the C-terminal loop mutants at -60 mV. **B.** Bottom and side view highlighting the CIRB domain and the electrostatic potential of this region.